Cirrus cloud thinning using a more physically-based ice microphysics scheme in the ECHAM-HAM GCM (acp-2021-685)

Colin Tully, David Neubauer, Nadja Omanovic, and Ulrike Lohmann

David Mitchell Review Author Response

Dear David,

Firstly, we would like to thank you for taking the time to review our study and provide detailed feedback on a specific area for improvement. Regarding the orographic component of the vertical velocity by Joos et al. (2008, 2010), it was excluded from the first submission, as in initial tests we believed we were double counting the TKE and orographic components of the vertical velocity in grid cells where orography was active. This resulted in high ICNC values that did not provide us with confidence in our results. It turned out this was not the case and was merely down to a numerical issue, related to parallelization, when using the parameterization in ECHAM6.3 with the new P3 ice microphysics scheme (Morrison and Milbrandt, 2015; Dietlicher et al. 2018, 2019). After reworking the code to make it compatible with P3 we could easily include this vertical velocity component in our simulations. However, after re-running the Full_D19 reference simulation to verify this new approach, we found that including the orographic component is not needed when using the P3 microphysics scheme. In this response we provide our findings that support this claim, and lay out a solution that is implemented in the revised manuscript.

In the manuscript we validate our model with the in-situ measurements by Krämer et al. (2020). Figure 1, below, shows the model validation comparison between our original model that is presented in the manuscript (P3 Ref) and the revised model including the orographic velocity component (P3 Oro) for the reference Full_D19 simulation. It is clear that this extra component has an impact on the modelled ICNC values at lower temperatures ($T < 215$ K). The model no longer captures the higher frequency of low ICNC values at these temperatures. Instead, the model median is about two orders of magnitude higher than the observed median value. The high frequency ICNC of 1000 L^{-1} around 205 K is not present in the in-situ measurements. Furthermore, at higher temperatures, the model also does not capture frequent low ICNC values.

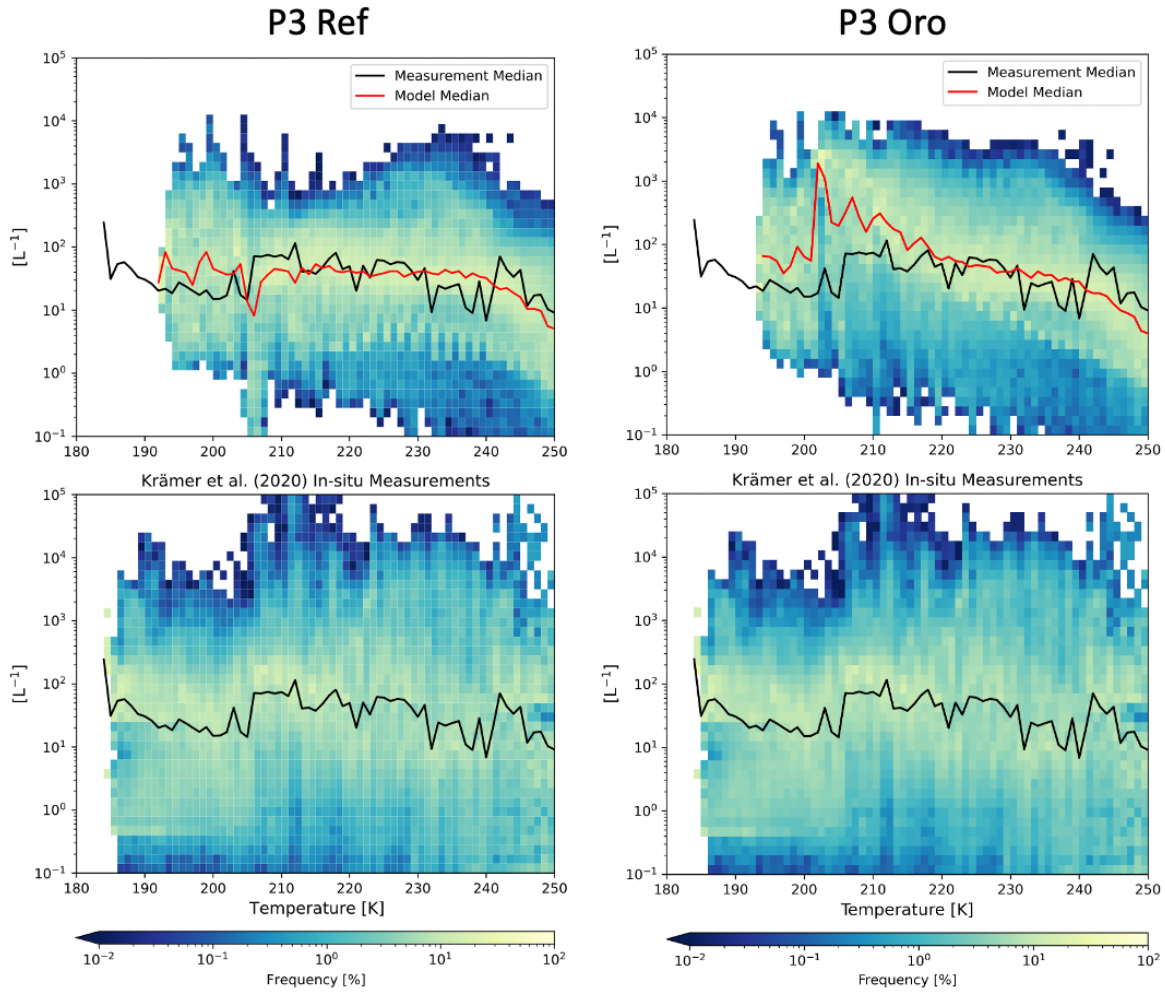

Figure 1: ICNC frequency diagrams for ice crystals with a diameter of at least 3 μm as a function of temperature between 180 K and 250 K binned like in Krämer et al. (2020) for every 1 K for P3 without the orographic velocity component (P3 Ref) and with the orographic velocity component (P3 Oro). The five-year global mean data from the model is plotted in the top row and the compilation of in-situ flight data from Krämer et al. (2020) is plotted in the bottom row. The red line in the upper plot represents the binned median ICNC value of the model data, and the black line in both plots is the same value for the observational data.

We examined this further by comparing our model to the DARDAR satellite remote-sensing ICNC dataset by Sourdeval et al. (2018) in Figure 2. Firstly, our model shows much wider ICNC variation than the DARDAR data for all temperature bins presented here. Muench and Lohmann (2020) note similar biases in their reference simulation associated with convective detrainment as well as the reduction of ice crystal sedimentation enhancement factors with their new cloud scheme. With the prognostic treatment of sedimentation with P3 (Dietlicher et al., 2018,2019), ice crystal removal is also slower and may contribute to high ICNC biases compared to DARDAR. Figure 3 shows the scatter of the modeled ICNC with and without the orographic component activated relative to the DARDAR ICNC dataset. We see that including the orographic component improves the correlation between the model and the satellite only between 223 and 233 K. For the colder temperature bins, activating the orographic velocity parameterization increases the root mean square error and worsens the correlation. However, the DARDAR data is not without its own biases that may not capture wider variability in the observed ICNC. Figure 4 from Krämer et

al. (2020) below shows the DARDAR retrieval frequency as well as ICNC percentiles for both the DARDAR dataset and the in-situ measurements. Firstly, it is noted that the majority of DARDAR measurements (~50%) are at temperatures > 225 K likely due to the overlapping occurrence of in-situ origin and liquid-origin cirrus clouds (Krämer et al., 2020; Wernli et al., 2016; Gasparini et al., 2018). However, what is important here is the variability of the ICNC values in the figure between the in-situ measurements (blue) and the DARDAR observations (red). Krämer et al. (2020) provide several reasons that explain the differences between the ICNC of these two observation platforms. Most notably is that DARDAR cannot detect the low ICNC associated with aged thin cirrus clouds at cold temperatures that were observed in the in-situ measurements. This is primarily due to insufficient sensitivity of the satellite instruments to these low ICNC values. A further bias originates from the assumptions made in the retrieval algorithm that is based on the parameterization by Delanoë et al. (2005) on particle size distribution (PSD) parameter constraints. As Sourdeval et al. (2018) note, this parameterization does not necessarily capture the multi-modality of the ice PSD observed in the in-situ measurements they compared in their study. This culminates in a potential overprediction of small ice crystals associated with high ICNC values at low temperatures that Krämer et al. (2020) explain is due to the transient nature of homogeneous nucleation and the complexities in observing this process in in-situ field campaigns. Finally, while our model shows more variability than the DARDAR data, likely as we can capture more regions of low ICNC at lower temperatures, it is within the range of the instantaneous in-situ measurement variability. In addition, by adding the orographic parameterization, high ICNC biases are enhanced due to the higher frequency of homogeneous nucleation, see below.

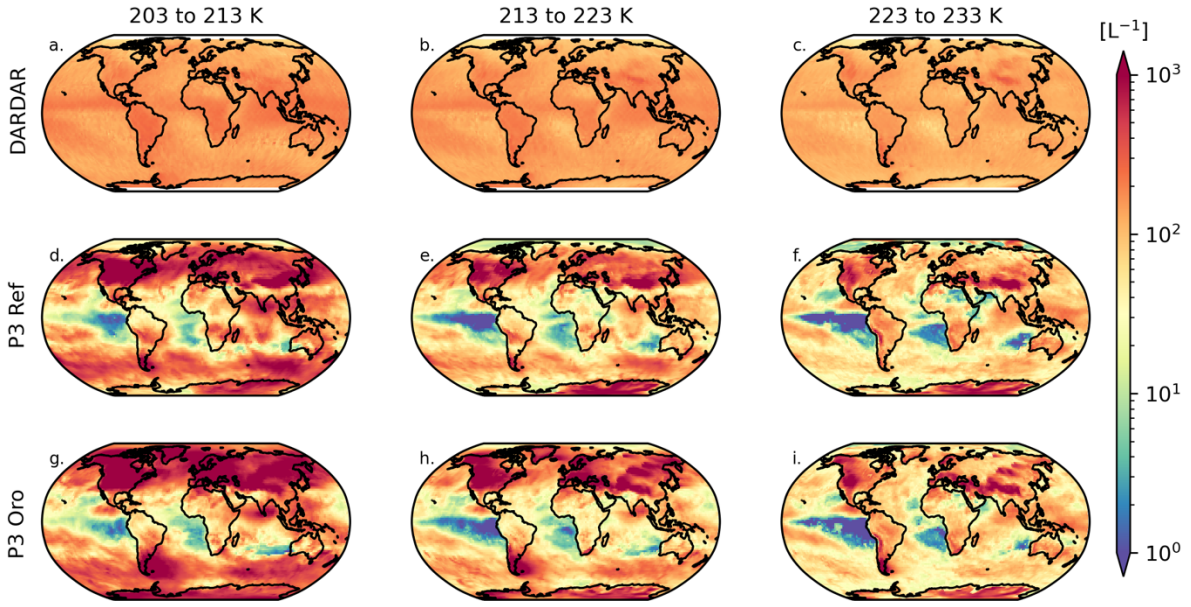

Figure 2: Spatial distribution of ICNC per DARDAR temperature bin. DARDAR data from Sourdeval et al. (2018) is plotted in a-c, 2010 annual mean model data without the orographic velocity component (P3 Ref) is plotted in d-f, and with the orographic velocity component in g-i.

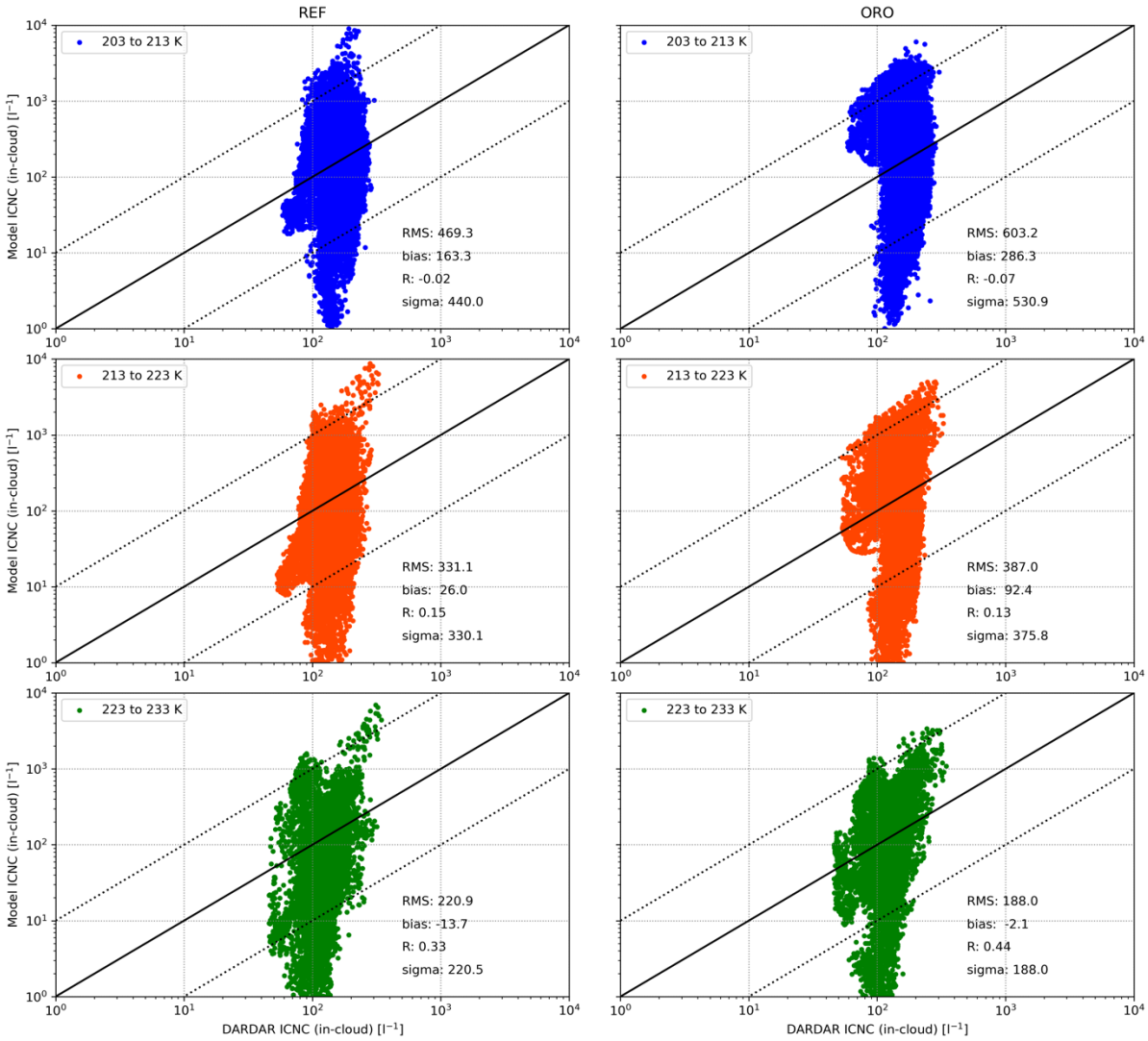

Figure 3: Adapted from Lohmann et al. (2020). Scatterplots of ICNC for the 2006-2016 annual mean DARDAR satellite remote-sensing dataset and the 2010 annual mean ECHAM-HAM ICNC for three DARDAR-defined temperature bins. The left column show the spread for the model without the orographic velocity component activated, and the right column the same but with the orographic component active. RMS is the root mean square error, R is the correlation coefficient, and sigma is the standard deviation of the difference between the modeled and satellite ICNC.

The key comparison is between P3 Ref (Figure 2d-f) and P3 Oro (Figure 2g-i). At the coldest temperatures between 203 and 213 K we find the highest mean ICNC values in our model for both P3 Ref and P3 Oro. In the former one can clearly see that mountainous regions around the Himalayas, the Andes, and the Rockies show local ICNC maxima. This is enhanced by adding the orographic velocity component in P3 Oro such that it weakens regional ICNC heterogeneity. In our P3 Ref simulation local ICNC maxima over mountainous regions become more apparent at higher temperatures, for example the elevated ICNC over Northern Chile and Southern Peru between 223 and 233 K (Figure 2f).

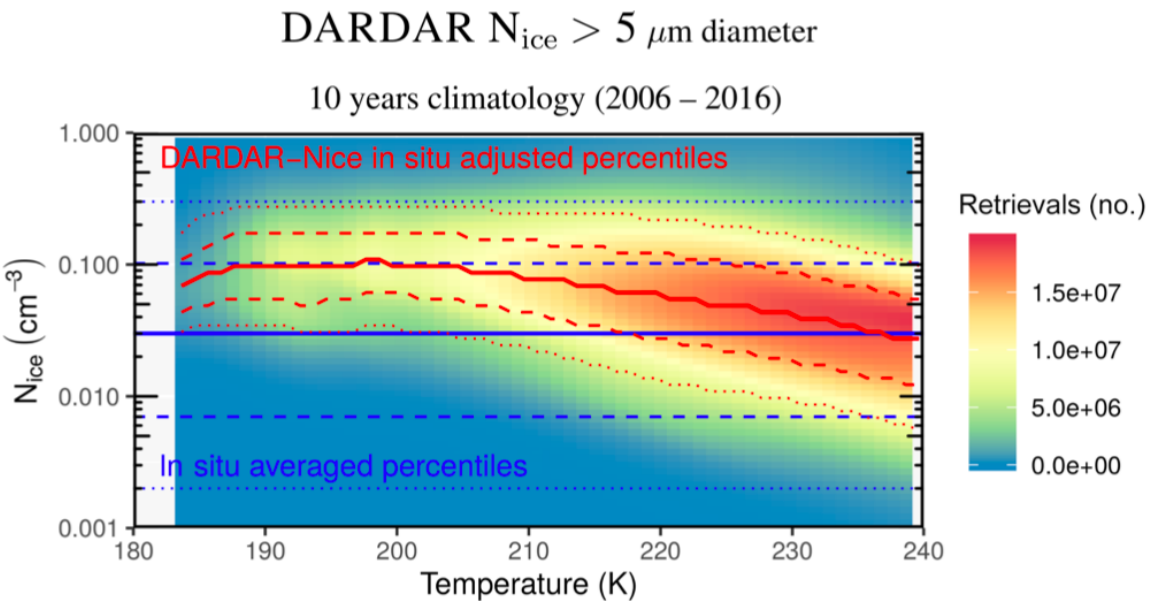

Figure 4: From Krämer et al. (2020). ICNC-temperature climatology. The colors in the background indicate the DARDAR retrieval frequency. The lines on the plot refer to the 10th and 90th (dotted), then 25th and 75th (dashed), and the 50th (solid) percentiles of DARDAR dataset (red) and the in-situ observations (blue).

Your main concern regarding our study as we understand it was that homogeneous nucleation within cirrus is underpredicted when excluding the orographic parameterization due to its strong dependence on vertical velocity. Figure 5 presents the ice number tracers at 200 hPa that were added to the model for this study. Like Figures 6 and 9 in the manuscript, these tracers represent the ice formed in-situ in the cirrus scheme that are then passed back to the microphysics scheme. Homogeneous nucleation forms the majority of in-situ cirrus ice in our model regardless of whether we include the orographic velocity component (Figure 5a and 5c). In fact, with this component activated homogeneous nucleation becomes more dominant, and like the DARDAR comparison above, some spatial heterogeneity is no longer evident. Heterogeneous nucleation also increases as critical ice saturation ratio values are reached more easily with the orographic component activated. Furthermore, Figure 6 is taken from Gasparini and Lohmann (2016) and shows the sources of cirrus ice using the default ECHAM microphysics scheme (2M) by Lohmann et al. (2007). Where heterogeneous nucleation was the dominant source of ice at 200 hPa for Gasparini and Lohmann (2016), that is not the case for our model with the P3 ice microphysics. Therefore, we argue that we do not underpredict homogeneous nucleation in in-situ cirrus in our model.

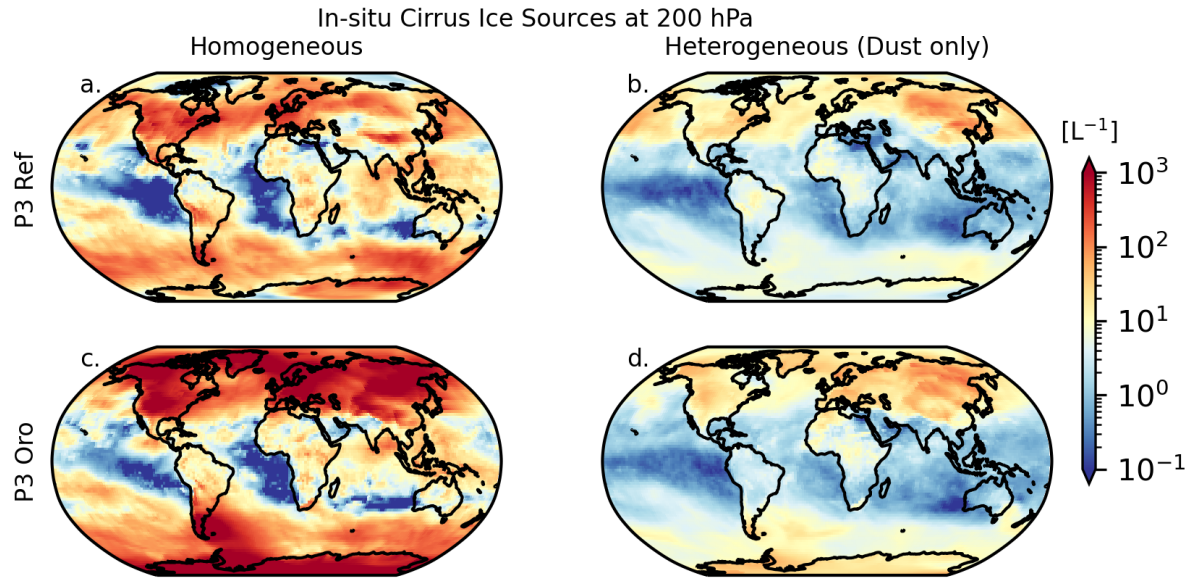

Figure 5: 2010 annual mean spatial distribution of in-situ ice number tracers on 200 hPa for the model without the orographic velocity component (a-b) and with the orographic velocity component (c-d).

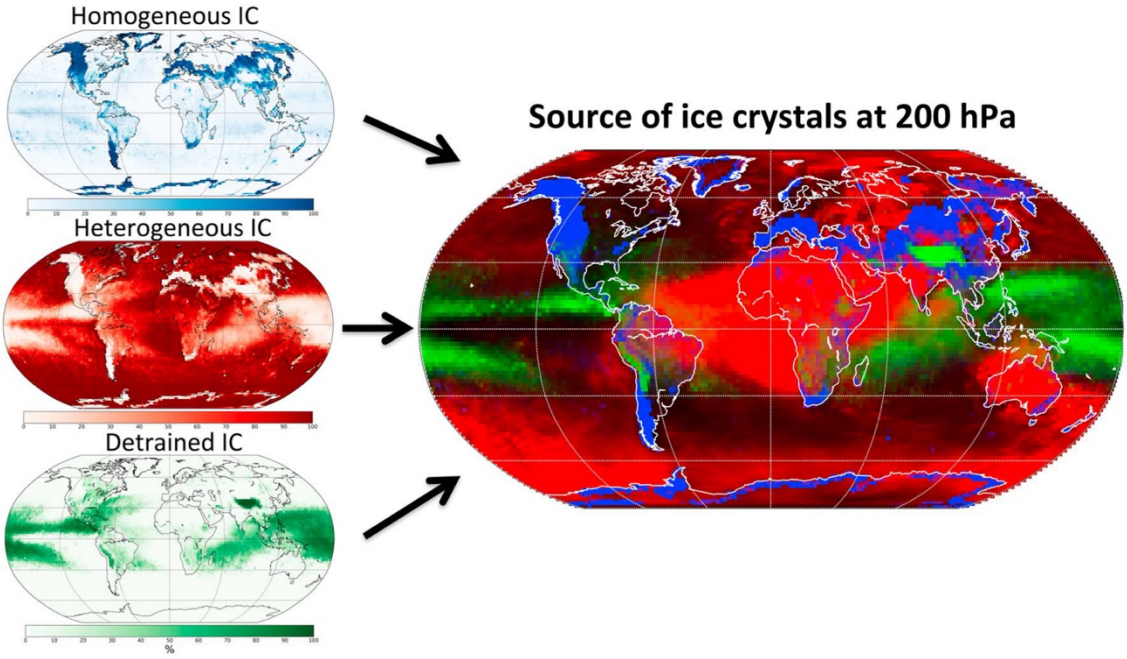

Figure 6: From Gasparini and Lohmann (2016), five year annual mean ice sources at 200 hPa for homogeneous nucleated ice, heterogeneously nucleated ice, and detrained ice crystals..

Based on the findings presented here, we conclude that the inclusion of the orographic velocity component is not needed with the P3 ice microphysics scheme. This highlights the fundamental difference between this newer microphysics scheme and the default ECHAM scheme (2M) by Lohmann et al. (2007) that was used in previous studies from our group (Gasparini and Lohmann, 2016; Gasparini et al., 2017). P3 utilizes prognostic sedimentation of ice hydrometeors by simulating the ice population using a single category, whereas the 2M scheme separates ice into two classes, in-cloud and precipitating. In order to maintain cloud-ice values and cloud radiative properties within the range of observations with the 2M scheme, ice

removal was sped up by enhancing ice crystal aggregation to form snow (Neubauer et al., 2019). This is no longer necessary with P3 as the size-class separation is no longer included in the model, and the updated cloud fraction scheme allows for fractional cirrus cloud cover above ice saturation. The result is much slower ice removal via sedimentation. We can clearly see the effects of this behavior in the plots presented here. Large ICNC values at the coldest temperatures (Figure 2d), originating predominantly from homogeneous nucleation (Figure 5a), are already achieved in our model. With the prognostic sedimentation in our model, these small ice crystals remain in the atmosphere for an extended period. The effect of the orographic velocity component is only to enhance homogeneous nucleation and form more ice that remains in the atmosphere for an even longer time period. We argue that while the orographic component was vital for ensuring homogeneous nucleation was not underpredicted when using the 2M scheme, it is no longer needed with the P3 scheme.

In conclusion, we excluded the orographic velocity component from our study based on our findings. However, as this is the first time the P3 ice microphysics scheme was validated with and without this component, we added an Appendix to the revised manuscript with the figures and explanations presented here.

Sincerely,
Colin Tully (on behalf of all co-authors)

References

- Delanoë, J., Protat, A., Testud, J., Bouniol, D., Heymsfield, A. J., Bansemer, A., Brown, P. R. A., and Forbes, R. M.: Statistical properties of the normalized ice particle size distribution, *Journal of Geophysical Research: Atmospheres*, 110, https://doi.org/https://doi.org/10.1029/2004JD005405, https://agupubs.onlinelibrary.wiley.com/doi/abs/10.1029/2004JD005405, 2005.
- Dietlicher, R., Neubauer, D., and Lohmann, U.: Prognostic parameterization of cloud ice with a single category in the aerosol-climate model ECHAM(v6.3.0)-HAM(v2.3), *Geoscientific Model Development*, 11, 1557–1576, https://doi.org/10.5194/gmd-11-1557-2018, https://gmd.copernicus.org/articles/11/1557/2018/, 2018.
- Dietlicher, R., Neubauer, D., and Lohmann, U.: Elucidating ice formation pathways in the aerosol–climate model ECHAM6-HAM2, *Atmospheric Chemistry and Physics*, 19, 9061–9080, https://doi.org/10.5194/acp-19-9061-2019, https://www.atmos-chem-phys.net/19/9061/ 2019/, 2019.
- Gasparini, B. and Lohmann, U.: Why cirrus cloud seeding cannot substantially cool the planet, *Journal of Geophysical Research: Atmospheres*, 121, 4877–4893, https://doi.org/10.1002/2015JD024666, https://agupubs.onlinelibrary.wiley.com/doi/abs/10.1002/ 2015JD024666, 2016.
- Gasparini, B., Münch, S., Poncet, L., Feldmann, M., and Lohmann, U.: Is increasing ice crystal sedimentation velocity in geoengineering simulations a good proxy for cirrus cloud seeding?, *Atmospheric Chemistry and Physics*, 17, 4871–4885, https://doi.org/10.5194/acp-17- 4871-2017, https://acp.copernicus.org/articles/17/4871/2017/, 2017.
- Gasparini, B., Meyer, A., Neubauer, D., Münch, S., and Lohmann, U.: Cirrus Cloud Properties as Seen by the CALIPSO Satellite and ECHAM-HAM Global Climate Model, *Journal of Climate*, 31, 1983–2003,

https://doi.org/10.1175/JCLI-D-16-0608.1, https://doi.org/10.835 1175/JCLI-D-16-0608.1, 2018.
- Joos, H., Spichtinger, P., and Lohmann, U.: Orographic cirrus in the global climate model ECHAM5, *Journal of Geophysical Research*, 113, https://doi.org/10.1029/2007JD009605, https://agupubs.onlinelibrary.wiley.com/doi/abs/10.1029/2007JD009605, 2008.
- Joos, H., Spichtinger, P., and Lohmann, U.: Influence of a future climate on the microphysical and optical properties of orographic cirrus clouds in ECHAM5, *Journal of Geophysical Research: Atmospheres,* 115, https://doi.org/https://doi.org/10.1029/2010JD013824, https: //agupubs.onlinelibrary.wiley.com/doi/abs/10.1029/2010JD013824, 2010.
- Krämer, M., Rolf, C., Spelten, N., Afchine, A., Fahey, D., Jensen, E., Khaykin, S., Kuhn, T., Lawson, P., Lykov, A., Pan, L. L., Riese, M., Rollins, A., Stroh, F., Thornberry, T., Wolf, V., Woods, S., Spichtinger, P., Quaas, J., and Sourdeval, O.: A microphysics guide to cirrus – Part 2: Climatologies of clouds and humidity from observations, *Atmospheric Chemistry and Physics*, 20, 12 569–12 608, https://doi.org/10.5194/acp-20-12569-2020, https://acp.copernicus.org/articles/20/12569/2020/, 2020.
- Lohmann, U., Stier, P., Hoose, C., Ferrachat, S., Kloster, S., Roeckner, E., and Zhang, J.: Cloud microphysics and aerosol indirect effects in the global climate model ECHAM5-HAM, Atmospheric Chemistry and Physics, 7, 3425–3446, https://doi.org/10.5194/acp-7-3425-2007, https://www.atmos-chem-phys.net/7/3425/2007/, 2007.
- Lohmann, U., Friebel, F., Kanji, Z., Mahrt, F., Mensah, A., and Neubauer, D.: Future warming exacerbated by aged-soot effect on cloud for- mation, Nature Geoscience, 13, 674–680, https://doi.org/10.1038/s41561-020-0631-0, https://doi.org/10.1038/s41561-020-0631-0, 2020.
- Morrison, H. and Milbrandt, J. A.: Parameterization of Cloud Microphysics Based on the Prediction of Bulk Ice Particle Properties. Part I: Scheme Description and Idealized Tests, Journal of the Atmospheric Sciences, 72, 287–311, https://doi.org/10.1175/JAS-D-14-0065.1, https://doi.org/10.1175/JAS-D-14-0065.1, 2015.
- Neubauer, D., Ferrachat, S., Siegenthaler-Le Drian, C., Stier, P., Partridge, D. G., Tegen, I., Bey, I., Stanelle, T., Kokkola, H., and Lohmann, U.: The global aerosol–climate model ECHAM6.3–HAM2.3 – Part 2: Cloud evaluation, aerosol radiative forcing, and climate sensitivity, *Geoscientific Model Development*, 12, 3609–3639, https://doi.org/10.5194/gmd-12-3609-2019, https://gmd.copernicus.org/articles/ 12/3609/2019/, 2019.
- Sourdeval, O., Gryspeerdt, E., Krämer, M., Goren, T., Delanöe, J., Afchine, A., Hemmer, F., and Quaas, J.: Ice crystal number concentration estimates from lidar--radar satellite remote sensing -- Part 1: Method and evaluation, *Atmospheric Chemistry and Physics*, 18, 14327-14350, https://doi.org/10.5194/acp-18-14327-2018, https://acp.copernicus.org/articles/18/14327/2018/, 2018.
- Wernli, H., Boettcher, M., Joos, H., Miltenberger, A.K., and Spichtinger, P.: A trajectory-based classification of ERA-Interim ice clouds in the region of the North Atlantic storm track, *Geophysical Research Letters*, 43, 6657-6664, https://doi.org/10.1002/2016GL068922, https://agupubs.onlinelibrary.wiley.com/doi/abs/10.1002/2016GL068922, 2016.